Direct Determination of Electron-Transfer Properties of Dicopper-Bound Reduced Dioxygen Species by a Cryo-Spectroelectrochemical Approach.

Isidoro López, Rui Cao, David A. Quist, Kenneth D Karlin, Nicolas Le Poul

ChemPubSoc Europe
DOI: 10.1002/chem.201705066
CHEMISTRY A European Journal
Full Paper

Redox Chemistry

Direct Determination of Electron-Transfer Properties of Dicopper-Bound Reduced Dioxygen Species by a Cryo-Spectroelectrochemical Approach.

Isidoro López,[a] Rui Cao,[b] David A. Quist,[b] Kenneth D. Karlin,*[b] and Nicolas Le Poul*[a]

Abstract: Direct experimental determination of redox properties of superoxo ($O_2^{\bullet-}$) and peroxo (O_2^{2-}) embedded in dicopper complexes bearing an unsymmetrical binucleating ligand was achieved using cryo-electrochemistry and cryo-spectroelectrochemistry in dichloromethane. Cyclic voltammetry for dicopper(I) ($\mathbf{1}^+$) oxidation to a $Cu^{I}Cu^{II}$ mixed-valent species ($\mathbf{1}^{2+}$) under inert atmosphere reveals slow heterogeneous electron-transfer kinetics, indicative of a large reorganization energy. Oxygenation of the dicuprous complex $\mathbf{1}^+$ gives the bridged peroxo dicopper(II) species $\mathbf{3}^+$, which is reversibly oxidized to the superoxo complex $\mathbf{2}^{2+}$ at $E^0 = 0.11$ V (vs. SCE) with a small inner sphere electron-transfer reorganization energy, $\lambda_i = 0.54$ eV, determined from variable temperature electrochemical impedance spectroscopy. The data suggest that the $O_2^{\bullet-}/O_2^{2-}$ redox process occurs directly on the O_2-derived core.

Molecular oxygen (O_2) is activated in chemical-catalytic systems or at the biological level by metal complexes or metalloenzymes through reduction processes that involve one or several active-site metal ions (Fe, Cu, Zn, Mn).[1] These processes lead to the formation of different metal–oxygen species such as superoxide, peroxide, hydroperoxide, and others (Scheme 1), which may have oxidative properties for oxygen atom insertion into C–H bonds.

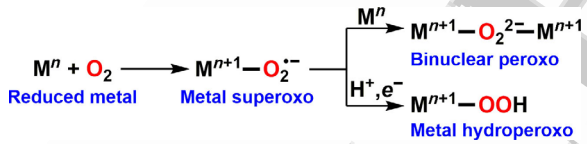

Scheme 1. O_2 reduction at reduced metal centers.

Most of these metal–oxygen species have a very short lifetime (ms) at room temperature making them difficult to be characterized. Although a good number of X-ray structures of copper–dioxygen complexes are now available,[2–8] there is still a great need for further fundamental information concerning Cu_n–O_2 electronic-structure/bonding, redox processes, and substrate oxygenation scope and mechanism of action. A great deal of information about structures and spectroscopic features of metal–oxygen centers can and have been obtained from synthetic models of enzymatic active sites by using fast-time acquisition set-ups, organic solvents, and low temperatures.[9] However, redox potentials and electron-transfer properties of such active species are scarce; that is, for products of O_2 stepwise reduction, in particular for copper–oxygen systems.[10,11] Nonetheless, such information is important for the development of efficient devices in the energy research area such as fuel cells (O_2-reduction), solar photoelectrochemical cells (water oxidation), and organic lithium–air batteries.[12]

Recent works have shown the possibility to indirectly estimate the redox potential of copper–oxygen species by using chemical oxidants.[13] Though attractive, this method requires the use of a large series of chemical reagents, and leads to an approximate value of the standard potential. Moreover, information about the reversibility of the electron transfer process (and associated kinetics) cannot be directly obtained from the experimental data. Hence, it appears as essential to be able to obtain direct measurements of the redox properties for metal–oxygen species. For that purpose, we have developed new cryo-electrochemical and UV/Vis-NIR cryo-spectroelectrochemical setups. Here, we have focused on the unsymmetrical $[Cu_2(UN\text{-}O^-)]^{2+/+}$ complexes $\mathbf{1}^{2+}$ and $\mathbf{1}^+$, which react with dioxygen and lead to the discrete superoxo and peroxo species $\mathbf{2}^{2+}$ and $\mathbf{3}^+$, respectively (Scheme 2).[13–15] These are only stable at low temperatures ($T < 200$ K) and the direct determination of their thermodynamic and kinetic redox properties, coupled to their authentic UV/Vis-NIR spectroscopic features, requires a novel cryo-spectroelectrochemical approach.

The redox behavior of $\mathbf{1}^+$ was first investigated by cyclic voltammetry (CV) at 293 K in dichloromethane under an inert atmosphere (Table 1). A first quasi-reversible system was detect-

[a] Dr. I. López, Dr. N. Le Poul
UMR CNRS 6521, Université de Bretagne Occidentale
6 Avenue Le Gorgeu, CS 93837, 29238 Brest Cedex 3 (France)
E-mail: nicolas.lepoul@univ-brest.fr
[b] Dr. R. Cao, D. A. Quist, Prof. K. D. Karlin
Department of Chemistry, Johns Hopkins University
Baltimore, Maryland 21218 (USA)
E-mail: karlin@jhu.edu
Supporting information and the ORCID identification number(s) for the author(s) of this article can be found under https://doi.org/10.1002/chem.201705066.

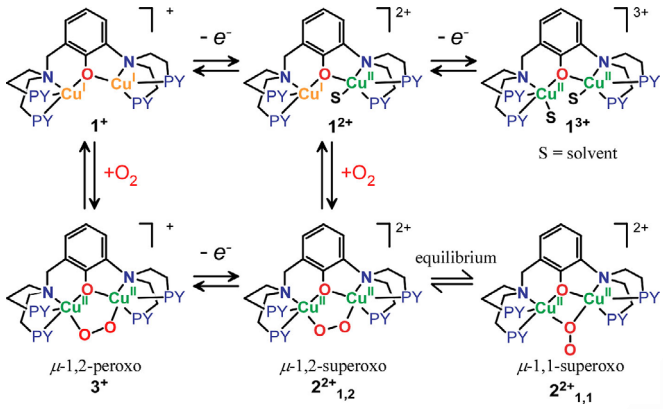

Scheme 2. Dicopper (UN-O⁻)-based complexes $\mathbf{1}^{+}$ and $\mathbf{1}^{2+}$ leading to peroxo $\mathbf{3}^{+}$ and superoxo $\mathbf{2}^{2+}$ species.

Table 1. Electrochemical data for $\mathbf{1}^{+}$, $\mathbf{1}^{2+}$, and $\mathbf{3}^{+}$ (0.5 mM) in CH_2Cl_2/NBu_4ClO_4 0.05 M ($v = 0.1\ V\,s^{-1}$).

Redox process	T [K]	E [V] vs. Fc	ΔE_p [mV]
$1^{2+} \rightleftharpoons 1^{+}$	293	$E^{0'}(1) = -0.31$	150
$1^{3+} \rightleftharpoons 1^{2+}$	293	$E^{0'}(2) = 0.03$	140
$1^{2+} \rightleftharpoons 1^{+}$	193	$E_{pa}(1) = 0.05$	1300
		$E_{pc}(1) = -1.46$	
$2^{2+} \rightleftharpoons 3^{+}$	193	$E^{0'}(4) = -0.36$	315

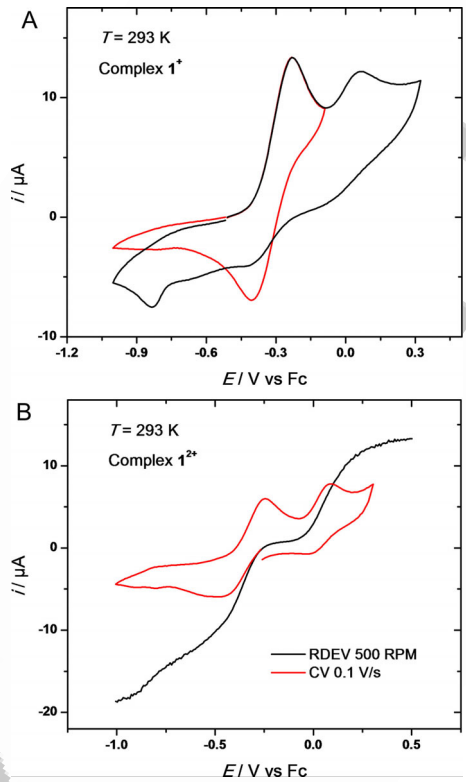

Figure 1. A) CVs ($v = 0.1\ V\,s^{-1}$) at $T = 293$ K of complex $\mathbf{1}^{+}$ (0.5 mM) under Argon, in CH_2Cl_2/NBu_4ClO_4 0.05 M (Pt WE). Red curve: $-1.0\ V < E < -0.1$ V vs. Fc; Black curve: $-1.0\ V < E < 0.35$ V vs. Fc. B) CV (red, 0.1 $V\,s^{-1}$) and RDEV (black, 500 RPM) of complex $\mathbf{1}^{2+}$ (0.4 mM) at 293 K in CH_2Cl_2/NBu_4ClO_4 0.05 M (Pt WE).

ed upon oxidation at $E^{0'}(1) = -0.31$ V vs. Fc with 150 mV peak separation (ΔE_p) (Table 1 and Figure 1 A, red curve). When scanning up to 0.5 V, a second system appeared at $E^{0'}(2) = 0.03$ V vs. Fc (Figure 1 A, black curve). The number of electrons, n, involved in the first redox process was obtained from the variation of the anodic peak current (i_{pa}) with square root of scan rate ($v^{1/2}$),[16] knowing the diffusion coefficient value of $\mathbf{1}^{+}$ from DOSY ^{1}H NMR experiments (Figures S2 and S3 in the Supporting Information). The value found for n (1 ± 0.1) clearly demonstrated that the process at $E^{0'}(1)$ is mono-electronic.

The same electrochemical experiments were carried out starting from the chemically synthesized complex $\mathbf{1}^{2+}$. CV and rotating-disk electrode voltammetry (RDEV) at 293 K showed that the complex can be reversibly oxidized at $E^{0'}(2)$ and reduced at $E^{0'}(1)$ (Figure 1 B) in agreement with the formation of dicopper (II,II) and (I,I) complexes, respectively. However, the mixed-valent complex $\mathbf{1}^{2+}$ was not indefinitely stable in solution at this temperature because the redox system at $E^{0'}(1)$ disappeared progressively, whereas a new one appeared at lower potential ($E^{0'}(3) = -0.85$ V) (Figure S4). This process was fully confirmed by RDEV (Figure S5). Complementary room-temperature UV/Vis-NIR spectroelectrochemical experiments were also performed in order to characterize the electrogenerated mixed-valent dicopper (I,II) $\mathbf{1}^{2+}$ species in solution starting from $\mathbf{1}^{+}$ (Figure S6). The spectra obtained upon oxidation did not display any intervalence charge transfer (IVCT) band in the 900–2000 nm region, as expected for a localized mixed-valent species (class I in the Robin–Day classification).[17] This data is in agreement with the previously published EPR spectrum of $\mathbf{1}^{2+}$, which showed a four line signal typical of a single copper(II) ion.[13,14]

Noteworthy, CV (0.1 $V\,s^{-1}$) of $\mathbf{1}^{+}$ at 193 K under a N_2 atmosphere displayed an oxidation peak at 0.05 V vs. Fc associated to a reduction peak at -1.46 V on the subsequent backscan (Figure 2 A, black curve). This behavior fully differs from that obtained at 293 K (Figure 1 A) and probably reflects large inner-sphere reorganizational effects affecting the electron-transfer kinetics at this temperature.

Dioxygen bubbling into a solution of $\mathbf{1}^{+}$ at 193 K led to immediate modification of the CV (Figure 2 A, orange curve). A new quasi-reversible system appeared at $E^{0'}(4) = -0.36$ V vs. Fc with $\Delta E_p = 315$ mV at $v = 0.1\ V\,s^{-1}$. Concomitantly, the oxidation peak at $E_{pa}(1)$ disappeared, confirming the full conversion of the complex to the peroxide complex $\mathbf{3}^{+}$. The intensity of the oxidation peak $i_{pa}(4)$ was almost identical to $i_{pa}(1)$, suggesting a monoelectronic process; that is, the peroxo- and superoxo-dicopper(II) complexes ($\mathbf{3}^{+}$ and $\mathbf{2}^{2+}$, respectively) are related by one-electron reversible redox interconversion. Variation of the scan rate (Figure 2 B) showed a linear dependence of $i_{pa}(4)$ with $v^{1/2}$ (Figure S7) and yielded $D_{193K} = 1.0 \times 10^{-6}\ cm^2\,s^{-1}$ if one assumes a mono-electronic oxidation.

On the other hand, it was previously shown by spectroscopic methods that oxygen addition to a cold (193 K) solution of the mixed-valence (II,I) complex $\mathbf{1}^{2+}$ affords the superoxo species $\mathbf{2}^{2+}$.[13] {Note: Previous spectroscopic interrogation of this

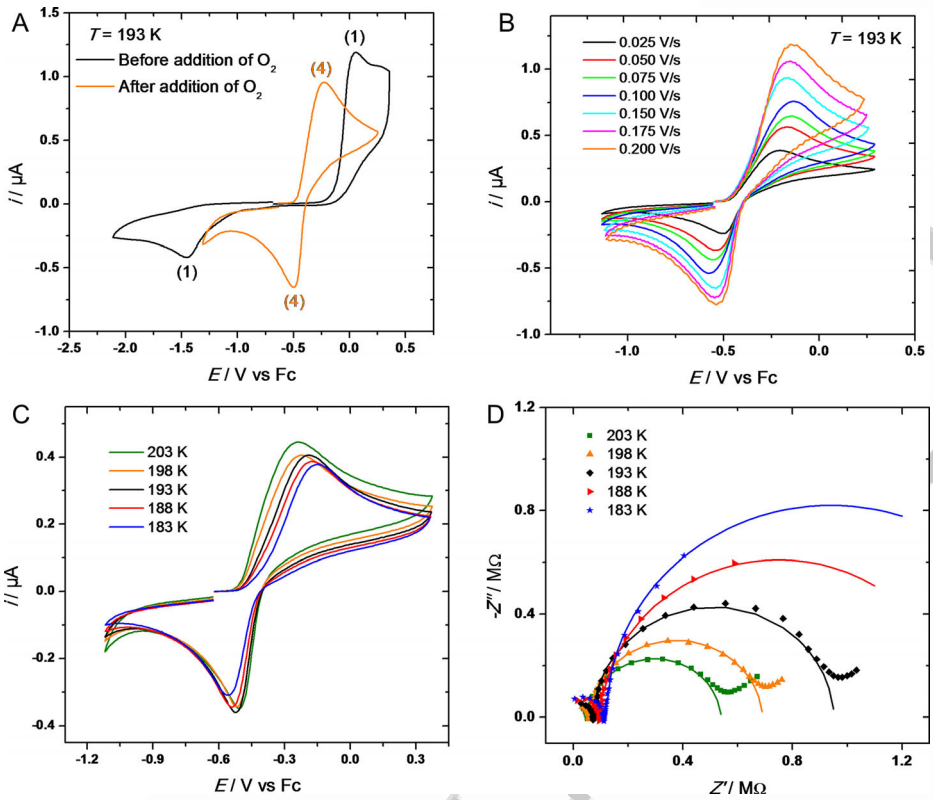

Figure 2. A) CVs ($v = 0.1$ V s^{-1}) at $T = 193$ K of complex $\mathbf{1}^+$ before (black) and after (orange) addition of dioxygen, in CH_2Cl_2/NBu_4ClO_4 0.05 M (Pt WE). B) CVs of complex $\mathbf{1}^+$ at various scan rate (0.025 V s^{-1} < v < 0.200 V s^{-1}) at $T = 193$ K after addition of dioxygen; C) CVs ($v = 0.1$ V s^{-1}) and D) Nyquist plots ($E_{app} = -0.36$ V vs. Fc, ac amplitude = 20 mV) of complex $\mathbf{3}^+$ (1 mM) in CH_2Cl_2/NBu_4ClO_4 0.05 M (Pt WE) for 183 K < T < 203 K. For the Nyquist plots, experimental values (symbols) were fit (solid lines) using the Randles equivalent circuit (see Figure S10 in the Supporting Information).

complex verified the superoxo-dicopper(II) formulation. EPR and resonance Raman spectroscopies indicated that the unpaired electron is localized on the superoxide ligand and that two isomers of $\mathbf{2}^{2+}$ are present in solution (Scheme 2)}.[13,14] This Cu_2:O_2 adduct is formally the one-electron oxidized species of the peroxo complex $\mathbf{3}^+$. Hence, complex $\mathbf{2}^{2+}$ was obtained from O_2 bubbling into a solution of $\mathbf{1}^{2+}$ in CH_2Cl_2/NBu_4ClO_4 0.05 M at 193 K. CV analysis of the superoxo $\mathbf{2}^{2+}$ displayed a quasi-reversible system, which is the same as that found for $\mathbf{3}^+$ at $E^0(4)$ ($\Delta E_p = 315$ mV), as clearly evidenced by the superposition of the two CVs by using the same internal redox reference (Ferrocene) (Figure S8).

According to previous spectroscopic studies,[13] these results strongly suggest that the redox process at $E^{0'}(4)$ is associated with the $\mathbf{2}^{2+}/\mathbf{3}^+$ superoxo/peroxo couple. Noticeably, the value of $E^{0'}(4)$ in CH_2Cl_2 (−0.36 V vs. Fc = 0.11 V vs. SCE) obtained by CV is very close to that previously determined by using a set of ferrocenyl oxidants (0.13 V vs. SCE).[13] When scanning over a wider potential window, no other oxidation process was detected except the solvent oxidation (Figure S9).

To fully confirm this result, time-resolved cryo-UV/Vis spectroelectrochemistry experiments were carried out under thin-layer conditions. Electrochemical oxidation of $\mathbf{3}^+$ led to the bleaching of the band at 508 nm and the appearance of a new one at 406 nm, which is indicative of the formation of the superoxo complex $\mathbf{2}^{2+}$ (Figure 3 A). Subsequent reduction at −0.6 V vs. Fc yielded back complex $\mathbf{3}^+$ in almost the same level (Figure 3 B). The same experiments were performed starting from the superoxo complex $\mathbf{2}^{2+}$: electrochemical reduction led to the decrease of the band at 406 nm and appearance of a new one at 508 nm (Figure 4 A). Further oxidation led back to the spectroscopic signature of $\mathbf{2}^{2+}$ (Figure 4 B). In both cases, an isosbestic point was detected at 441 nm, consistent with the reversible $\mathbf{2}^{2+}/\mathbf{3}^+$ direct interconversion (Figures 3 and 4), and confirming that the system at $E^{0'}(4)$ corresponds to the $\mathbf{2}^{2+}/\mathbf{3}^+$ couple.

Electrochemical analyses were pursued by variation of the temperature between 183 K and 203 K. As shown in Figure 2 C for CVs, the decrease of the temperature induced a larger peak separation, as expected for lowering of the standard electron transfer rate constant (k^0), as well as lower peak current values, as a result of slower mass transfer. In order to get access to the kinetics of electron transfer (k^0), electrochemical impedance spectroscopy (EIS)[16] was also carried out. Each EIS spectrum (Nyquist plots, Figure 2 D) was fit by considering a classical Randles equivalent circuit for the electrochemical cell (Figure S10).[16] This circuit involves a solution resistance term (R_{unc}), and a charge-transfer impedance term (comprising charge-transfer resistance R_{ct} and double-layer capacitance C_{dl}). Good matches between experimental Nyquist plots and fitted curves were obtained (Figure 2 D). This allowed the determination of the standard heterogeneous rate constant k^0 from R_{ct}

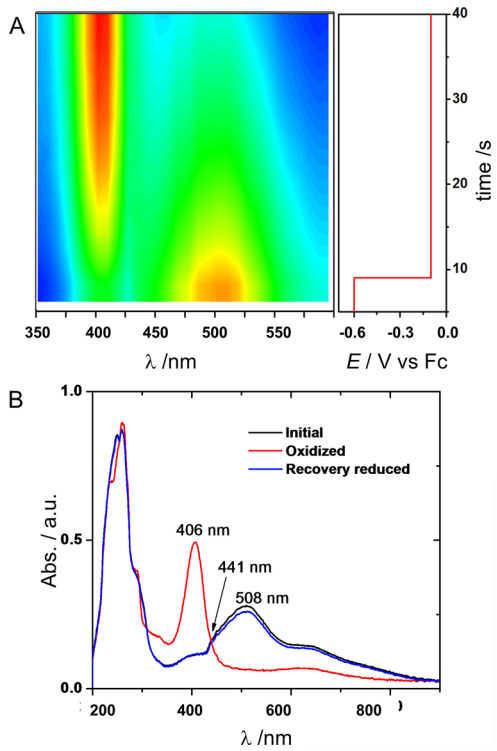

Figure 3. A) Time-resolved UV/Vis monitoring of the electrochemical oxidation of complex $\mathbf{3}^+$ ($E_{app}=-0.10$ V vs. Fc, red curve) at $T=193$ K, in CH_2Cl_2/NBu_4ClO_4 0.05 M (Pt WE) by using a cryo-spectroelectrochemical cell (optical path: 0.2 mm). Colors display the absorbance value from blue (Abs = 0) to red (Abs = 0.5); B) Low-temperature (193 K) UV/Vis spectra obtained by electrochemical oxidation at $E_{app}=-0.10$ V vs. Fc of complex $\mathbf{3}^+$ (red curve), then reduction (−0.6 V, blue curve), in CH_2Cl_2/NBu_4ClO_4 0.05 M (Pt WE).

for each temperature (see Table 2), according to Equation (1):[16,18,19]

$$R_{ct} = \frac{RT}{n^2F^2Ak^0C_{ox}^{(1-\alpha)}C_{red}^{(\alpha)}} \quad (1)$$

where R = gas constant, T = temperature, n = number of electrons transferred, F = Faraday constant, A = electrode area, and α = transfer coefficient, whereas C_{ox} and C_{red} are oxidized and reduced species concentrations, respectively.

A plot of ln [k^0] versus T^{-1} is linear, as expected for a thermally activated process (Figure 5), yielding the activation free energy ΔG^*_{exp} (23.1 kJ mol^{-1}) and a pre-exponential factor A'

Table 2. Values of solution resistance (R_{unc}), charge-transfer resistance (R_{ct}), double-layer capacitance (C_{dl}), and standard rate constant (k^0) obtained from EIS on a solution of complex $\mathbf{3}^+$ (1 mM) in CH_2Cl_2/NBu_4ClO_4 0.05 M (Pt WE) for 183 K < T < 203 K according to the Randles equivalent circuit described in Figure S10. For calculations of k^0, see Equation (1).

T [K]	R_u [kΩ]	C_{dl} [nF]	R_{ct} [kΩ]	10^6 k^0 [cm s^{-1}]
183	112.210	16.605	1850.50	16.4
188	94.596	30.860	1320.10	23.8
193	73.937	41.550	891.96	36.4
198	60.072	40.728	626.58	53.5
203	53.617	40.541	488.33	70.8

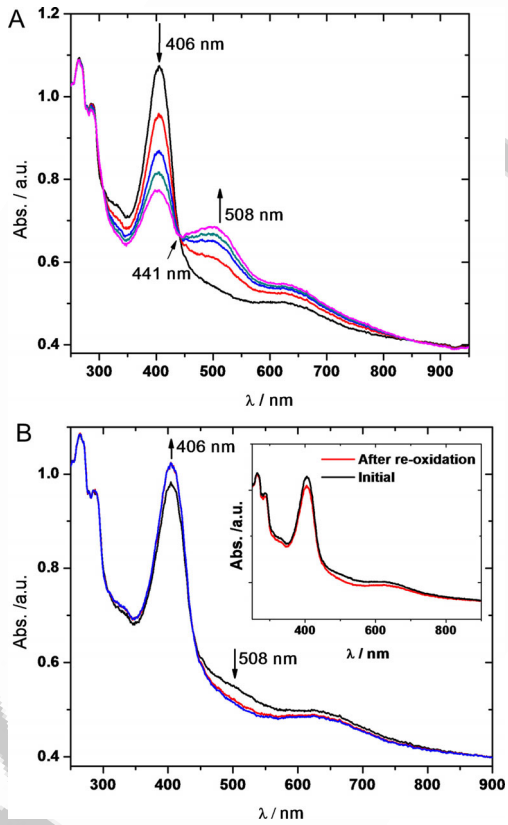

Figure 4. Low-temperature (193 K) UV/Vis monitoring of the electrochemical A) reduction at $E_{app}=-0.6$ V vs. Fc, then B) subsequent oxidation at $E_{app}=-0.1$ V of complex $\mathbf{2}^{2+}$ in CH_2Cl_2/NBu_4ClO_4 0.05 M (Pt WE) by using a cryo-spectroelectrochemical cell (optical path: 0.2 mm). Inset panel B: comparison of UV/Vis spectra before (initial, black) and after (red) reduction and oxidation.

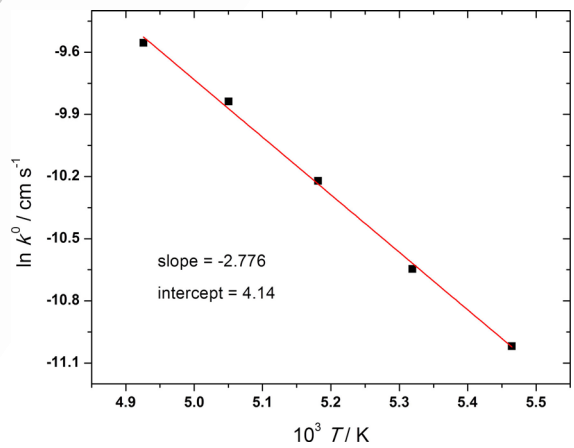

Figure 5. Plots of ln k^0 vs. T^{-1} obtained from analysis of EIS data for complex $\mathbf{3}^+$ in CH_2Cl_2/NBu_4ClO_4 0.05 M (Pt WE) for 183 K < T < 203 K (see Table 2 for k^0 values).

(64 cm s^{-1}). Extrapolation of the linear curve gave the standard rate constant at 298 K, $k^0_{298\,K}=0.006$ cm s^{-1}. For comparison, this value is 40 times larger than that found for [Cu(TMPA)(H_2O)]$^{2+/+}$ in dry DCM by the same approach (1.4×10^{-4} cm s^{-1}).[19] The reorganization energy of the electron-trans-

fer process, λ_{exp}, was then calculated from the activation free energy ΔG^*_{exp}. We found that $\lambda_{exp} = 0.95$ eV, which is consistent with the value previously determined from homogeneous electron transfer of the $\mathbf{2}^{2+}/\mathbf{3}^{+}$ redox couple using ferrocenyl redox reagents (0.84 eV).[13]

The outer-sphere reorganization energy (λ_0) for the redox process was then calculated using the Born dielectric continuum model, by assuming that the distance between the electrode and the complex is much larger than the complex radius, according to Equation (2):[16]

$$\lambda_o = \frac{N_A e_0^2}{4\pi\varepsilon_0}\left(\frac{1}{a_0}\right)\left(\frac{1}{\varepsilon_{op}} - \frac{1}{\varepsilon_s}\right) \quad (2)$$

where N_A = Avogadro constant, e_0 = fundamental electronic charge, ε_0 = permittivity of free space, and a_0 = complex's mean radius, whereas ε_{op} and ε_s are the optical and static dielectric constant of the medium, respectively.

Calculations give $\lambda_0 = 0.41$ eV, thus leading to λ_i since $\lambda_i = \lambda_{exp} - \lambda_0 = 0.54$ eV. This value is similar to that previously calculated by DFT for the superoxo-peroxo system (0.4 eV).[13] The relatively low value of λ_i is consistent with only very slight modifications of bond lengths and angles within the complex upon electron exchange. In agreement with DFT calculations that were previously carried out for this superoxo/peroxo redox couple,[13] it is reasonable to ascertain that the electron-transfer processes only involve the superoxide/peroxide moieties, and not the copper metal ions or the phenolate group. As a consequence, the thermodynamic ($E^{0\prime} = 0.11$ V vs. SCE) and kinetic ($k^0_{298\,K} = 0.006$ cm s^{-1}) features characterize redox interconversions of the superoxide/peroxide ($O_2^{\bullet-}/O_2^{2-}$) pair where the $O_2^{\bullet-}/O_2^{2-}$ moieties are embedded in a pre-organized dicupric core. Such a situation is rendered possible by the topology of the ligand; the phenoxide bridge as well as the two aza cores induce sufficient constraints to maintain both Cu^{I} ions at a short distance (approximatively 3.65 Å).[13–15] This allows incorporation of dioxygen in a favored manner, and oxidation of the cuprous ions without significant modification of the backbone.

Regarding the formal potential value, we have compared our data with analogous peroxo-bridged dicobalt(III) complexes.[10c] Their formal potential ranges between 0.51 and 0.69 V vs. Fc, about 900 mV more positive than the value found for $\mathbf{2}^{2+}/\mathbf{3}^{+}$. This indicates that complex $\mathbf{3}^{+}$ displays higher electron density on the peroxide core than its cobalt analogues, despite similar *N*-donor environment. As previously discussed,[13] this derives from stronger electron-withdrawing effects of the dicobalt(III) core assuming that charge at the HOMO is localized on the dioxygen core for both peroxo complexes. Interestingly, superoxo/peroxo dicopper complexes bearing a dinucleating pyrazolate-bridged bis(tacn) (tacn = triazacyclononane) ligand have been very recently studied at much higher temperature (273 K) in acetonitrile by CV.[11] A quasi-reversible system was found at −0.59 V vs. Fc and ascribed to a ligand-centered redox process according to UV/Vis spectroscopic experiments driven by chemical reagents. The lower value of $E^{0\prime}$ (−0.59 V vs. Fc) for the tacn system compared to the $\mathbf{2}^{2+}/\mathbf{3}^{+}$ redox couple (−0.36 V) can be reasonably assigned due to the better donor effect of the tacn ligand.

In conclusion, the cryoelectrochemical studies demonstrated dramatic changes upon addition of dioxygen to either $\mathbf{1}^{+}$ or $\mathbf{1}^{2+}$. The results imply that a very large reorganization energy is involved in $\mathbf{1}^{+} \rightarrow \mathbf{1}^{2+}$, whereas the peroxide $\mathbf{3}^{+}$ to superoxide $\mathbf{2}^{2+}$ oxidation is kinetically facile. Noteworthy is that the $E^{\circ\prime}$ value for the $O_2^{\bullet-}/O_2^{2-}$ redox couple lies close to the physiological range, as previously mentioned.[13] Future short-term work will focus on the effect of ligand symmetry/constraint/substituents for this well-developed family of dicopper complexes with bound superoxide, peroxide, or hydroperoxide.[20] Moreover, the newly-developed cryo-spectroelectrochemical setup will be useful for the characterization of more reactive complexes (e.g., ferryl or cupryl) that catalyze the C–H bond activation of organic compounds.

Acknowledgements

Financial support by ANR-13-BSO7-0018, Conseil Général du Finistère, and Université de Bretagne Occidentale. K.D.K. acknowledges support from the USA N.I.H. (GM028962).

Conflict of interest

The authors declare no conflict of interest.

Keywords: copper · cyclic voltammetry · oxygen reduction/evolution · reduction potential · reorganization energy

[1] a) E. I. Solomon, D. E. Heppner, E. M. Johnston, J. W. Ginsbach, J. Cirera, M. Qayyum, M. T. Kieber-Emmons, C. H. Kjaergaard, R. G. Hadt, L. Tian, *Chem. Rev.* **2014**, *114*, 3659–3853; b) Y. Sheng, I. A. Abreu, D. E. Cabelli, M. J. Maroney, A. F. Miller, M. Teixeira, J. S. Valentine, *Chem. Rev.* **2014**, *114*, 3854–3918; c) T. L. Poulos, *Chem. Rev.* **2014**, *114*, 3919–3962.

[2] S. T. Prigge, B. A. Eipper, R. E. Mains, L. M. Amzel, *Science* **2004**, *304*, 864–867.

[3] J. P. Bacik, S. Mekasha, Z. Forsberg, A. Y. Kovalevsky, G. Vaaje-Kolstad, V. G. H. Eijsink, J. C. Nix, L. Coates, M. J. Cuneo, C. J. Unkefer, J. C. Chen, *Biochemistry* **2017**, *56*, 2529–2532.

[4] K. A. Magnus, B. Hazes, H. Ton-That, C. Bonaventura, J. Bonaventura, W. G. Hol, *Proteins* **1994**, *19*, 302–309.

[5] Y. Matoba, T. Kumagai, A. Yamamoto, H. Yoshitsu, M. Sugiyama, *J. Biol. Chem.* **2006**, *281*, 8981–8990.

[6] Y. Li, Y. Wang, H. Jiang, J. Deng, *Proc. Natl. Acad. Sci. USA* **2009**, *106*, 17002–17006.

[7] Synthetic model system crystal structures exist for peroxo-Cu^{II}_2, superoxo-Cu^{II}, peroxo-Cu^{II}, and $Cu^{III}_2(\mu\text{-}O)_2$ complexes. See refs. [1a] and [9].

[8] There are a number of X-ray structures for multicopper (four ions) oxidases containing a reduced dioxygen species surrounded by three Cu ions; there may be issues surrounding the interpretation of X-ray data, due to radiation damage. See the discussion in ref. [1a].

[9] a) C. E. Elwell, N. L. Gagnon, B. D. Neisen, D. Dhar, A. D. Spaeth, G. M. Yee, W. B. Tolman, *Chem. Rev.* **2017**, *117*, 2059–2107; b) M. Costas, M. P. Mehn, M. P. Jensen, L. Que, Jr., *Chem. Rev.* **2004**, *104*, 939–986; c) L. M. Mirica, X. Ottenwaelder, T. D. Stack, *Chem. Rev.* **2004**, *104*, 1013–1045; d) J. J. Liu, D. E. Diaz, D. A. Quist, K. D. Karlin, *Isr. J. Chem.* **2016**, *56*, 738–755; e) D. A. Quist, D. E. Diaz, J. J. Liu, K. D. Karlin, *J. Biol. Inorg. Chem.* **2017**, *22*, 253–288.

[10] a) N. M. Carvalho, O. A. Antunes, A. Horn, Jr., *Dalton Trans.* **2007**, 1023–1027; b) N. Ségaud, E. Anxolabehere-Mallart, K. Senechal-David, L. Acosta-Rueda, M. Robert, F. Banse, *Chem. Sci.* **2015**, *6*, 639–647; c) M. S.

Vad, F. B. Johansson, R. K. Seidler-Egdal, J. E. McGrady, S. M. Novikov, S. I. Bozhevolnyi, A. D. Bond, C. J. McKenzie, *Dalton Trans.* **2013**, *42*, 9921–9929; d) R. L. Peterson, J. W. Ginsbach, R. E. Cowley, M. F. Qayyum, R. A. Himes, M. A. Siegler, C. D. Moore, B. Hedman, K. O. Hodgson, S. Fukuzumi, E. I. Solomon, K. D. Karlin, *J. Am. Chem. Soc.* **2013**, *135*, 16454–16467; e) D. Dhar, W. B. Tolman, *J. Am. Chem. Soc.* **2015**, *137*, 1322–1329.

[11] N. Kindermann, C. J. Gunes, S. Dechert, F. Meyer, *J. Am. Chem. Soc.* **2017**, *139*, 9831–9834.

[12] a) Z. Lyu, Y. Zhou, W. Dai, X. Cui, M. Lai, L. Wang, F. Huo, W. Huang, Z. Hu, W. Chen, *Chem. Soc. Rev.* **2017**, *46*, 6046–6072; b) D. G. Kwabi, V. S. Bryantsev, T. P. Batcho, D. M. Itkis, C. V. Thompson, Y. Shao-Horn, *Angew. Chem. Int. Ed.* **2016**, *55*, 3129–3134; *Angew. Chem.* **2016**, *128*, 3181–3186; c) P. G. Bruce, S. A. Freunberger, L. J. Hardwick, J. M. Tarascon, *Nat. Mater.* **2011**, *11*, 19–29.

[13] R. Cao, C. Saracini, J. W. Ginsbach, M. T. Kieber-Emmons, M. A. Siegler, E. I. Solomon, S. Fukuzumi, K. D. Karlin, *J. Am. Chem. Soc.* **2016**, *138*, 7055–7066. DFT calculations were carried out and confirm the superoxo-dicopper(II) formulation of $\mathbf{2}^{2+}$.

[14] M. Mahroof-Tahir, K. D. Karlin, *J. Am. Chem. Soc.* **1992**, *114*, 7599–7601.

[15] M. Mahroof-Tahir, N. N. Murthy, K. D. Karlin, N. J. Blackburn, S. N. Shaikh, J. Zubieta, *Inorg. Chem.* **1992**, *31*, 3001–3003.

[16] A. J. Bard, L. R. Faulkner, *Electrochemical Methods: Fundamentals and Applications*, 2nd ed., Wiley, **2001**.

[17] M. B. Robin, P. Day, *Adv. Inorg. Chem. Radiochem.* **1968**, *10*, 247–422.

[18] N. Le Poul, S. J. Green, Y. Le Mest, *J. Electroanal. Chem.* **2006**, *596*, 47–56.

[19] A. G. Porras Gutiérrez, J. Zeitouny, A. Gomila, B. Douziech, N. Cosquer, F. Conan, O. Reinaud, P. Hapiot, Y. Le Mest, C. Lagrost, N. Le Poul, *Dalton Trans.* **2014**, *43*, 6436–6445.

[20] a) K. D. Karlin, Z. Tyeklar, A. Farooq, M. S. Haka, P. Ghosh, R. W. Cruse, Y. Gultneh, J. C. Hayes, P. J. Toscano, J. Zubieta, *Inorg. Chem.* **1992**, *31*, 1436–1451; b) N. N. Murthy, M. Mahroof-Tahir, K. D. Karlin, *Inorg. Chem.* **2001**, *40*, 628–635; c) L. Li, A. A. Sarjeant, K. D. Karlin, *Inorg. Chem.* **2006**, *45*, 7160–7172.

Manuscript received: October 25, 2017
Accepted manuscript online: October 26, 2017
Version of record online: ■■ ■■, 0000

FULL PAPER

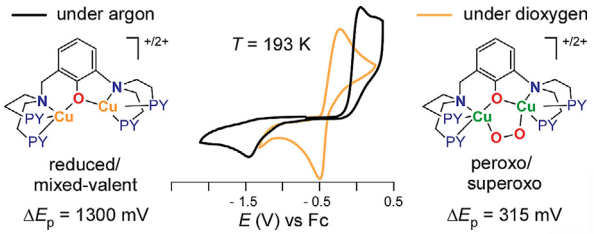

Peroxo/superoxo interconversion: O_2^{2-} and O_2^{-} interactions with metal ions are important in O_2-reduction or metal-mediated oxidations. Here, superoxo or peroxo (O_2^{-}/O_2^{2-})■■$O_2^{\bullet-}/O_2^{2-}$ in main text■■ moieties bound to a dicupric ion center are shown to interconvert and a reduction potential is determined (by cryo-spectroelectrochemistry) as 0.11 V (vs. SCE). Other electrochemical techniques allow determination of a very low inner-sphere reorganization energy of $\lambda_i = 0.54$ eV, indicating that the electron-transfer is localized on the O_2^{-}/O_2^{2-}■■ core.

Redox Chemistry

I. López, R. Cao, D. A. Quist, K. D. Karlin, N. Le Poul**

■■ – ■■

Direct Determination of Electron-Transfer Properties of Dicopper-Bound Reduced Dioxygen Species by a Cryo-Spectroelectrochemical Approach.

Karlin et al. @JohnsHopkins @UBO UnivBrest on electrochemical analysis of peroxo/superoxo redox properties SPACE RESERVED FOR IMAGE AND LINK

Share your work on social media! *Chemistry - A European Journal* has added Twitter as a means to promote your article. Twitter is an online microblogging service that enables its users to send and read text-based messages of up to 140 characters, known as "tweets". Please check the pre-written tweet in the galley proofs for accuracy. Should you or your institute have a Twitter account, please let us know the appropriate username (i.e., @accountname), and we will do our best to include this information in the tweet. This tweet will be posted to the journal's Twitter account @ChemEurJ (follow us!) upon online publication of your article, and we recommended you to repost ("retweet") it to alert other researchers about your publication.

Please check that the ORCID identifiers listed below are correct. We encourage all authors to provide an ORCID identifier for each coauthor. ORCID is a registry that provides researchers with a unique digital identifier. Some funding agencies recommend or even require the inclusion of ORCID IDs in all published articles, and authors should consult their funding agency guidelines for details. Registration is easy and free; for further information, see http://orcid.org/.

Dr. Isidoro López
Dr. Rui Cao
David A. Quist
Prof. Kenneth D. Karlin http://orcid.org/0000-0002-5675-7040
Dr. Nicolas Le Poul http://orcid.org/0000-0002-5915-3760